



# Accuracy of three dimensional-planned patient-specific instrumentation in femoral and tibial rotational osteotomy for patellofemoral instability

Lukas Jud<sup>1</sup> · Lazaros Vlachopoulos<sup>1</sup> · Silvan Beeler<sup>1</sup> · Timo Tondelli<sup>1</sup> · Philipp Fümstahl<sup>2</sup> · Sandro F. Fucentese<sup>1</sup>

Received: 2 December 2019 / Accepted: 30 January 2020 / Published online: 13 February 2020  
© SICOT aisbl 2020

## Abstract

**Purpose** Patellofemoral instability can be caused by tibial or femoral torsional deformity. Established surgical treatment options are rotational osteotomies, but the transfer from pre-operative planning to surgical execution can be challenging. Patient-specific instruments (PSI) are proofed to be helpful tools in realignment surgery. However, accuracy of PSI in femoral and tibial rotational osteotomies remains still unknown. Goal of the present study was to evaluate the accuracy of PSI in femoral and tibial rotational osteotomies in a patient population suffering from patellofemoral instability.

**Methods** All patients that underwent femoral or tibial rotational osteotomy using PSI in case of patellofemoral instability from October 2015 until April 2019 in our clinic were included. Twelve knees with twelve supracondylar femoral and seven supratuberositary tibial rotational osteotomies could be included. Accuracy of the correction was assessed using pre- and post-operative CT scans based on conventional measurements and, in 3D, based on 3D bone models of the respective patients.

**Results** CT measurements revealed an absolute difference between planned and achieved rotation of  $4.8^\circ \pm 3.1^\circ$  for femoral and  $7.9^\circ \pm 3.7^\circ$  for tibial rotational osteotomies without significant difference ( $p = 0.069$ ). Regarding 3D assessment, a significant difference could be observed for the residual error between femoral and tibial rotational osteotomies in the 3D angle ( $p = 0.014$ ) with a higher accuracy for the femoral side.

**Conclusion** The application of PSI for femoral and tibial rotational osteotomy is a safe surgical treatment option. Accuracy for femoral rotational osteotomies is higher compared with tibial rotational osteotomies using PSI.

**Keywords** Torsional deformity · Rotational osteotomy · Knee osteotomy · Torsional malalignment syndrome · Femoral osteotomy · Tibial osteotomy

✉ Lukas Jud  
lukas.jud@balgrist.ch

Lazaros Vlachopoulos  
vlachopoulos@balgrist.ch

Silvan Beeler  
silvan.beeler@balgrist.ch

Timo Tondelli  
timo.tondelli@balgrist.ch

Philipp Fümstahl  
philipp.fuernstahl@balgrist.ch

Sandro F. Fucentese  
sandro.fucentese@balgrist.ch

<sup>1</sup> Balgrist University Hospital, Department of Orthopedics, University of Zurich, Forchstrasse 340, 8008 Zürich, Switzerland

<sup>2</sup> Research in Orthopedic Computer Science (ROCS), University Hospital Balgrist, University of Zurich, Zurich, Switzerland

## Introduction

Patellofemoral instability is often multifactorial and can be caused by frontal malalignment of the leg, dysplastic trochlea, disruption of the medial soft tissue, patella alta, or torsional deformity of the femur or tibia [1, 2]. In case of a torsional deformity, femoral or tibial rotational osteotomy may be necessary [1–4]. However, an unintended change of the frontal mechanical leg axis is an identified problem in femoral rotational osteotomies [5, 6]. Appropriate pre-operative planning can be helpful in preventing such unintended malalignment [7], but accurate implementation of the planned osteotomy planes in the surgery can be challenging due to the limited surgical exposure and following potential mal-angulation of the osteotomy planes further aggravate deviations of the post-operative frontal mechanical leg axis [8]. Possible navigation aids are patient-specific instruments (PSI). Regarding the

application of PSI on the femur and the tibia, it has already been proofed to be helpful in coronal realignment surgery [9–11]. However, the accuracy of PSI in femoral or tibial rotational osteotomy has not been investigated so far. Goal of this study was to assess the accuracy of PSI in femoral and tibial rotational osteotomy in a patient population suffering from patellofemoral instability by pre- and post-operative radiological assessment in CT and three-dimensional (3D) assessment by the use of 3D bone models of the respective patients.

## Materials and methods

All patients that underwent femoral and/or tibial rotational osteotomy using PSI in case of patellofemoral instability from October 2015 to April 2019 in our clinic were included. In total, 12 knees (six right and six left knees) from ten mature patients (all female) with 12 supracondylar femoral and seven supratuberositary tibial rotational osteotomies could be included (Fig. 1). Average age at time of surgery

was 24 years (range 15 to 40 years). All knees showed a positive patellar apprehension test and all but two knees showed recurrent patellar luxation. Ten knees had a dysplastic trochlea. Caton-Deschamps index was in mean  $1.2 \pm 0.2$  (range 0.8 to 1.5). In all but one knee, additional reconstruction of the medial patellofemoral ligament was performed. In seven knees additional trochleoplasty, and in three knees additional lengthening of the lateral retinaculum was performed. In four out of five knees without tibial rotational osteotomy, an osteotomy and medial transfer of the tibial tuberosity was conducted due to an increased tibial tuberosity-trochlear groove distance of  $20.7 \pm 4.0$  mm (range 16.8 to 24.7 mm). For pre-operative planning, all patients had a computed tomography (CT) scan of the affected lower extremity, scanning the regions of interest including the proximal femur, distal femur, proximal tibia, distal tibia, distal fibula, and the talus. For assessment of the osteotomy, likewise a CT scan of the extremity, using the same CT protocol, was performed in mean at six months follow-up (range 3 to 15 months). For assessment of activity and patellofemoral instability, pre- and post-operative Tegner and Kujala scores were collected.

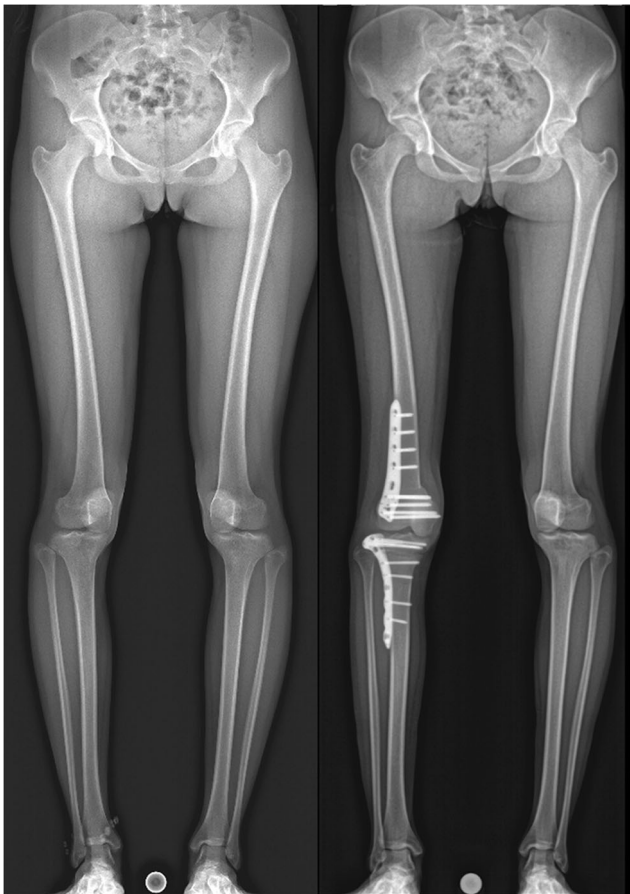
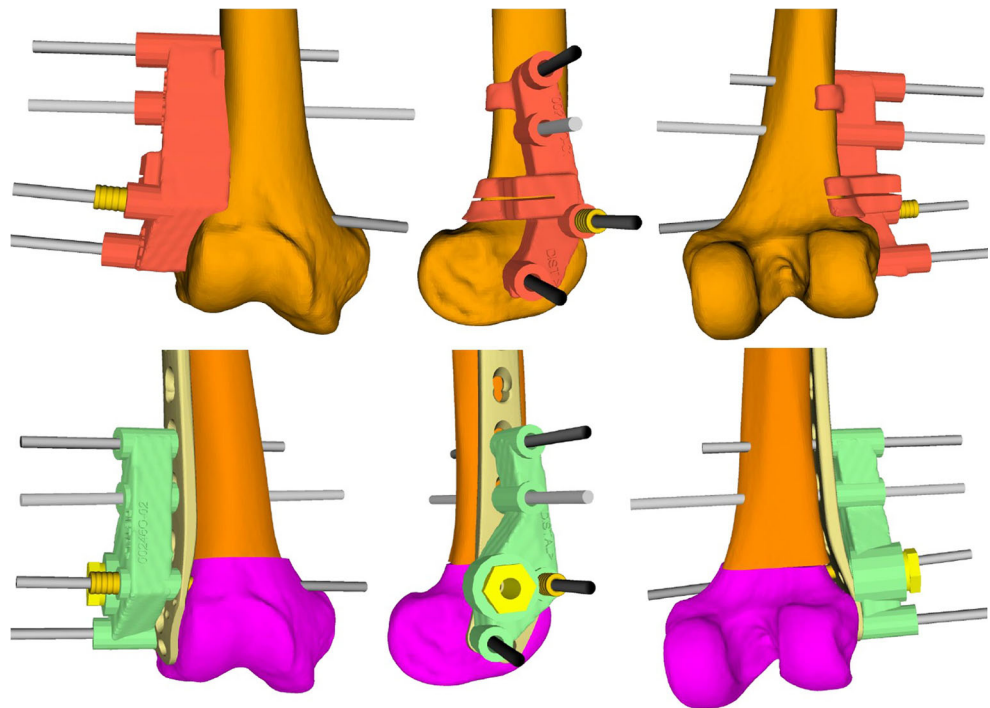


**Fig. 1** Long leg radiographs of a patient that underwent supracondylar femoral and supratuberositary tibial rotational osteotomy. On the left side the pre-operative situation, on the right side 3 months post-operatively

## Pre-operative osteotomy planning and PSI generation

Using pre-operative CT data, triangular surface models of the lower extremities were generated. The bone models were imported into the in-house developed computer-aided design (CAD) surgical planning software CASPA (Balgrist CARD, Zurich, Switzerland). As a first step, the supracondylar femoral external rotating osteotomy was simulated perpendicular to the mechanical femoral axis, in a way that a Tomofix Lateral Distal Femur Plate (Depuy-Synthes Oberdorf, Switzerland) could be properly placed. As a first PSI, the pre-reduction PSI was designed, containing drill holes for the reference pins (serving for registration of the following PSI) and the cutting slit for the supracondylar osteotomy. Next, the external rotation of the distal femoral fragment was simulated in mean with an external rotation of  $19.3^\circ$  (range  $14^\circ$  to  $27^\circ$ ). As a second PSI, the post-reduction PSI was designed using the reference pins to control for the planned rotation. Placement of the post-reduction PSI was planned together with the Tomofix Lateral Distal Femur Plate (Fig. 2). Next, if needed, the supratuberositary tibial internal rotating osteotomy was simulated perpendicular to the mechanical tibial axis, in a way that a VA-LCP Proximal Tibial Plate (Depuy-Synthes Oberdorf, Switzerland) could be properly placed. Afterwards, planning for the pre- and the post-reduction PSI for the supratuberositary osteotomy was performed in a same manner as for the supracondylar osteotomy with a mean internal rotation of the distal tibial fragment of  $20.4^\circ$

**Fig. 2** PSI for the supracondylar femoral rotational osteotomy. In the upper row the pre-reduction PSI in red, containing the reference pins (gray) and the cutting slit. In the lower row the post-reduction PSI in green, using the same reference pins to control for correct reduction. The Tomofix Lateral Distal Femur Plate in gold is placed over the predrilled screw holes



(range 15° to 25°) and placement of the VA-LCP Proximal Tibial Plate together with the post-reduction PSI.

The designed PSI were manufactured by Medacta International S.A. (Castel San Pietro, Switzerland).

### Surgical technique

The senior surgeon (FS) performed all surgeries. Using a subvastus approach for the femur, respectively using an approach through the anterior compartment of the lower leg for the tibia, the distal and lateral femur, respectively the proximal and lateral tibia, were relieved from soft tissue to identify prominent bony landmarks that have been integrated in the undersurface of the PSI for proper PSI positioning. Next, the pre-reduction PSI was positioned, screw positions for the Tomofix Lateral Distal Femur Plate respectively for the VA-LCP Proximal Tibial Plate were drilled using the integrated drill sleeves, and the respective osteotomy was performed using the integrated cutting slit. After placing the post-reduction PSI together with the Tomofix Lateral Distal Femur Plate, respectively, the VA-LCP Proximal Tibial Plate over the reference pins, the predefined rotation was performed and the screws were successively inserted. Finally, plate position and reduction were controlled by fluoroscopy.

### Aftercare

For a period of six weeks, patients were allowed for partially weight bearing with 15 kg. First follow-up was scheduled at six weeks post-operatively with standard radiographs of the

knee. To confirm bony consolidation, CT scans were obtained at three months post-operatively earliest.

### Assessment of the surgical execution accuracy

Femoral torsion was measured in pre- and post-operative CT according to the method described by Waidelich et al. [12]. The achieved femoral rotation was calculated as the difference between the pre-operative and the post-operative femoral torsion.

The tibial torsion was measured in pre- and post-operative CT according to the method described by Goutallier et al. [13]. The achieved tibial rotation was calculated as the difference between the pre- and the post-operative tibial torsion.

Using post-operative CT data, likewise triangular surface models of the lower extremities were generated in a same manner as with the pre-operative CT data and the pre- and post-operative bone models were imported into CASPA. 3D accuracy assessment was then performed using a similar methodology as described by Vlachopoulos et al. [14]. Using the 3D surface models, the post-operative proximal femur and the distal femoral shaft, respectively the post-operative tibial plateau (proximal from the osteotomy) were aligned with the pre-operative planning using Iterative Closest Point (ICP) surface registration algorithm (Fig. 3) [15, 16]. Afterwards, the difference between planned and achieved reduction was measured in all six degrees of freedom by computing the difference between the pre-operative planning and the post-operative distal femur, respectively, the post-operative tibial shaft including the distal tibia (distal from

**Fig. 3** Post-operative three-dimensional (3D) accuracy assessment by calculation of the residual error. **a** The post-operative bone models (violet) were superimposed with the pre-operative planned reduction (orange) proximal from the osteotomy (i.e., proximal femur and distal femoral shaft, respectively tibial plateau). **b** The residual deviation from the pre-operative planning is calculated by superimposition of the post-operative fragments distal from the osteotomy (green) with the pre-operative planned reduction (orange) (i.e., distal femur, respectively tibial shaft and distal tibia)

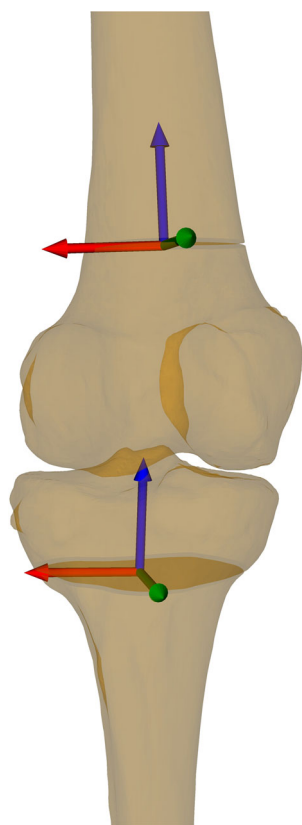
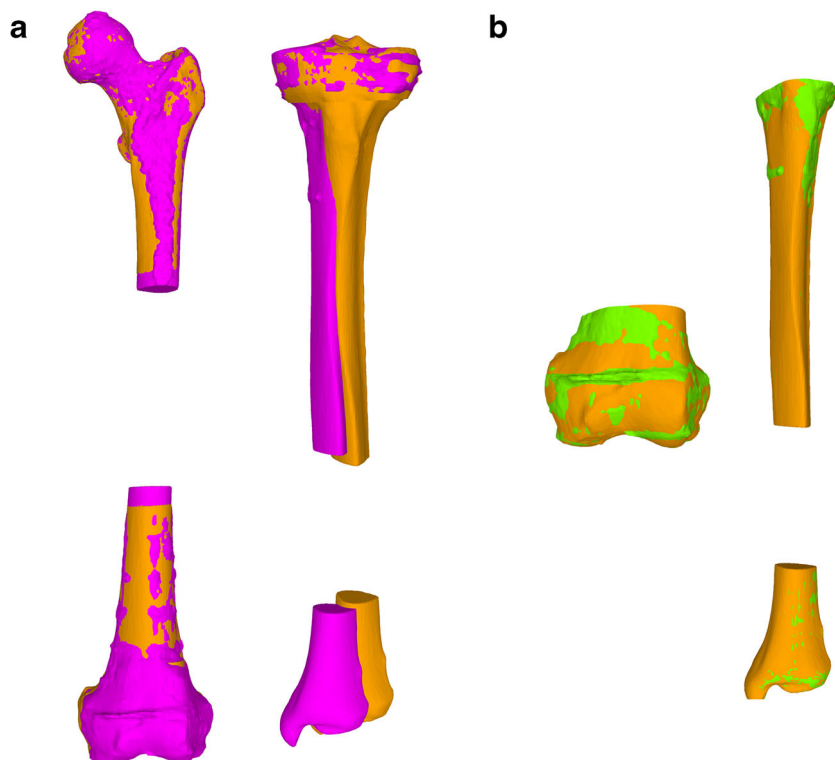


**Fig. 4** Standardized coordinate systems in the centre of the osteotomies. Green the x-axis (frontal plane), blue the y-axis (axial plane), red the z-axis (sagittal plane). Difference of rotation was noted according to these three axes as well as translational error

the osteotomy). Measurements were performed with respect to a standardized coordinate system in the centre of the respective osteotomy (Fig. 4), defined according to the International Society of Biomechanics (ISB) [17]. The difference of rotation was noted in axis-angle representation (3D angle) and as three consecutive rotations additionally (i.e., Euler rotations), according to the residual rotational error [18]. The rotations corresponded to the frontal plane (x-axis), the axial plane (y-axis), and the sagittal plane (z-axis). The translational error was also expressed as three consecutive values along the three axes according to the residual translational error.

The 3D mechanical leg axis was measured antero-posterior (AP) projected, using a similar method as described by Frnstahl et al. [19]. The difference between the pre- and the post-operative mechanical leg axis was calculated.

For inter-rater reliability, all femoral and tibial torsion measurements in CT, accuracy measurements in 3D, and mechanical leg axis measurements were performed by two independent readers (JL, BS).

### Statistical analysis

Inter-rater reliability was calculated using the interclass correlation coefficient (ICC), absolute agreement, two-way random effects model. Interclass correlation coefficients were interpreted according to Landis and Koch [20]. For the remaining analyses, mean values of both raters were used. Accuracy of the osteotomies was assessed by the absolute

**Table 1** Pre- and post-operative Tegner and Kujala scores. Mean values, standard deviation, and range (square brackets) are noted

	Pre-OP	Post-OP	<i>p</i> value
Tegner score	3.7 ± 0.9 [2–5]	3.7 ± 1.0 [2–6]	0.818
Kujala score	72.9 ± 12.8 [47–90]	81.8 ± 15.8 [49–98]	0.007

values of the deviations. Due to the sample size, the differences were analyzed by non-parametric tests. Signed-rank tests were used to compare pre- to post-operative clinical scores. Tibial and femoral deviations from the planned rotations were compared by Mann-Whitney *U* tests. If not stated otherwise, mean and standard deviation were presented. Statistical analyses were computed using Stata/IC 15.1 (StataCorp LP, College Station, TX, USA).

## Results

No surgery had intra- or peri-operative complications and all osteotomies were regularly consolidated. However, in one case mobilization of the knee in short general anaesthesia was necessary three months post-operatively due to a restricted range of motion with a knee-flexion of merely 15 degrees. After seven months, the patient was able to gain the range of motion back to a flexion of 115 degrees. No further complications occurred.

An overview of pre- and post-operative Tegner and Kujala scores is given in Table 1. The average follow-up was 11 ± six months. A significant difference could be noted for the Kujala score (*p* = 0.007). Regarding the post-operative patellar apprehension test, all but one knee showed no longer a positive patellar apprehension test.

An overview of the pre- and post-operative femoral and tibial torsion measured in CT is given in Table 2. Regarding the absolute difference between planned and achieved rotation, no significant difference between femoral and tibial rotational osteotomies could be observed (*p* = 0.069).

An overview of the post-operative accuracy measurements in 3D, respectively the residual errors, is given in Table 3. Regarding the mean difference between the tibial and femoral

residual errors, a significant difference could be observed for the 3D angle (*p* = 0.014).

Mean pre-operative mechanical leg axis was 1.3° varus ± 1.8° (range 4.8° varus to 1.1° valgus) and changed to a mean post-operative mechanical leg axis of 0.1° valgus ± 2.6° (range 4.4° varus to 3.5° valgus). The absolute mean difference between pre- and post-operative mechanical leg axis was 2.5° ± 1.4° (range 0.4° to 4.6°).

ICC between two readers showed to be “almost perfect” for mechanical leg axis [0.974 (95% CI 0.941–0.989)], femoral torsion [0.966 (95% CI 0.923–0.985)], and tibial torsion [0.967 (95% CI 0.916–0.987)]. ICC for the 3D angle of the femoral rotational osteotomies showed to be “substantial” [0.779 (95% CI 0.415–0.930)] and for the tibial rotational osteotomies it showed to be “almost perfect” [0.991 (95% CI 0.950–0.998)].

## Discussion

The most important finding of this study is that the application of PSI in femoral and tibial rotational osteotomies in patients suffering from patellofemoral instability caused by femoral and/or tibial rotational deformity is a safe surgical treatment option. No intra- or peri-operative complications could be observed. Likewise, even with only a short-term follow-up, a significant improvement could be observed for the Kujala score and all but one knees no longer showed a positive patellar apprehension test. Regarding the current literature for the use of PSI in femoral rotational osteotomy, Fiz et al. performed a femoral diaphyseal rotational osteotomy in a post-traumatic femoral rotational deformity using 3D printed surgical guides but without a statement about the surgical accuracy [21]. Concerning the use of PSI in tibial rotational osteotomy, Dobbe et al. experimentally evaluated the accuracy of tibial rotational osteotomy using PSI and showed an accuracy of ≤ 1.1° in their plastic bone model [22]. Otherwise, the application of PSI in femoral or tibial rotational osteotomy received little attention in the current literature so far. Regarding the evaluated accuracy in this study, no significant difference between femoral and tibial rotational osteotomies was noted in the CT measurements. However, regarding the residual error in 3D, a significant difference could be observed with a higher

**Table 2** Accuracy assessment measured in CT. Mean values, standard deviation, and range (square brackets) for pre- and post-operative femoral and tibial torsion. Positive values for femoral torsion stand for anteversion, positive values for tibial torsion stand for external rotation.

	Pre-OP torsion	Post-OP torsion	Achieved rotation	Planned rotation	Abs. difference planned–achieved rotation
Femur	42.3° ± 7.5° [31.7°–52.4°]	21.8° ± 6.5° [13.1°–33.1°]	20.5° ± 5.8° [8.2°–30.6°]	19.3° ± 4.7° [14.0°–27.0°]	4.8° ± 3.1° [0.4°–10.4°]
Tibia	35.3° ± 7.5° [27.1°–47.8°]	22.9° ± 7.3° [13.8°–32.2°]	12.5° ± 3.3° [9.6°–17.3°]	20.4° ± 3.6° [15°–25°]	7.9° ± 3.7° [2.8°–14.2°]

Furthermore noted is the achieved rotation whereby for the femur the rotation stands for external rotation and for the tibia for internal rotation of the distal fragment. Next the planned rotation is noted and the absolute difference between planned and achieved rotation

**Table 3** 3D accuracy assessment of the residual error from planned to achieved correction. Mean values, standard deviation, and range (square brackets) are noted. The residual error is described as 3D angle (axis-angle representation) and by Euler rotations around the standardized

coordinate system in the center of the osteotomy. Residual translation is also given with respect to the standardized coordinate system. Values are based on absolute values. In the lower row, mean difference between tibial and femoral residual error, including *p* value, is given

	3D (°)	Rotation (°)			Translation (mm)		
		Frontal plane (x-axis)	Axial plane (y-axis)	Sagittal plane (z-axis)	Frontal plane (x-axis)	Axial plane (y-axis)	Sagittal plane (z-axis)
Femur	5.4 ± 2.7 [1.8–10.2]	2.3 ± 1.5 [0.6–5.6]	3.2 ± 3.6 [0.3–9.5]	1.9 ± 1.8 [0.2–5.5]	2.3 ± 1.5 [0.0–5.2]	1.8 ± 1.2 [0.5–4.4]	1.2 ± 1.2 [0.1–4.2]
Tibia	10.3 ± 4.4 [5.0–18.6]	1.7 ± 2.0 [0.1–5.2]	4.8 ± 5.6 [0.4–16.8]	3.9 ± 2.5 [0.5–6.9]	1.0 ± 0.4 [0.6–1.8]	0.9 ± 1.0 [0.2–2.9]	0.9 ± 0.8 [0.0–2.1]
Mean Difference ( <i>p</i> value)	4.9 (0.014)	− 0.6 (0.204)	1.6 (0.398)	2.0 (0.063)	− 1.3 (0.128)	− 0.9 (0.076)	− 0.3 (0.673)

accuracy in femoral rotational osteotomies. While on the femoral side in some cases an overcorrection compared with the pre-operative planning could be observed, in all tibial rotational osteotomies an undercorrection was noted. Probably the main reason for this circumstance is the fibula that acts like a locking mechanism during internal tibial rotation and wherefore some authors propose to perform an additional fibula osteotomy in case of an intended tibial rotational correction of > 20° [23]. However, there exists still controversy about the need for an additional fibula osteotomy and opponents mention the better stability, that might also be reflected in the lower 3D residual translational error observed in tibial rotational osteotomies compared with the femoral osteotomies in this study, and the lower morbidity when avoiding the additional fibula osteotomy, whereby the proponents argue with a stress-free rotation by using the fibula osteotomy [24, 25]. Regarding the 3D residual rotational error, the issue about stress-free rotation could also be reflected in this study. Even though it was most marked in the axis corresponding to the reduction task (y-axis) for both procedures, it was still more pronounced on the tibial side with the named locking mechanism of the fibula. The less pronounced 3D residual rotational errors in the remaining axes probably can be explained as a result of a combination of the imprecise reduction task and a slightly incorrect positioning of the PSI, caused by insufficient adaption of the PSI on the bones or remaining underlying soft tissue. Regarding the mechanical leg axis, the absolute mean difference between the pre- and the post-operative mechanical leg axis, in this study population with complex deformity correction, was comparable with the observed accuracy of high tibial osteotomy in the current literature [26].

One of the main limitations of this study is the lack of a control group that has been operated upon with the conventional technique. Reason therefore is that we perform these complex procedures exclusively with the aid of PSI since we have this new technology at hand. Before the availability of PSI, unfortunately, the post-operative radiological datasets of the patients were not standardized like nowadays in our clinic,

and wherefore a control group was not possible. Likewise, regarding the current literature, the accuracy of tibial or femoral rotational osteotomies have not been investigated radiologically so far, neither with the conventional technique nor with the aid of PSI. However, it has to be assumed even without a control group that the evaluated accuracy in this study is probably higher than with the conventional technique, as it has already been shown in coronal realignment surgeries that the application of PSI lever up the surgical accuracy [9–11]. Another limitation is the short follow-up of the patients and that the clinical scores were not collected all at the same time post-operatively. However, the main focus of this study was the accuracy of femoral and tibial rotational osteotomies and the successful clinical results of such procedures have already been described in the literature [3, 4]. Lastly, the limited sample size in this study has to be mentioned, and this could be a reason why no significant difference in the CT measured accuracy between femoral and tibial rotational osteotomies was observed.

## Conclusion

The application of PSI for femoral and tibial rotational osteotomy in patellofemoral instability is a safe surgical treatment option. Accuracy for femoral rotational osteotomies is higher compared to tibial rotational osteotomies using PSI.

## Compliance with ethical standards

**Conflict of interest** All authors declare that they have no conflict of interest.

**Ethical approval** The local ethical committee approved this study (Zurich Cantonal Ethics Committee, KEK 2018–02242) and all patients gave their informed consent for their participation in and the publication of this study.

## References

- Hinterwimmer S, Rosenstiel N, Lenich A, Waldt S, Imhoff AB (2012) Femoral osteotomy for patellofemoral instability. *Unfallchirurg* 115(5):410–416. <https://doi.org/10.1007/s00113-012-2198-8>
- Nelitz M, Dreyhaupt J, Williams SR, Dornacher D (2015) Combined supracondylar femoral derotation osteotomy and patellofemoral ligament reconstruction for recurrent patellar dislocation and severe femoral anteversion syndrome: surgical technique and clinical outcome. *Int Orthop* 39(12):2355–2362. <https://doi.org/10.1007/s00264-015-2859-7>
- Drexler M, Dwyer T, Dolkart O, Goldstein Y, Steinberg EL, Chakraverty R, Cameron JC (2014) Tibial rotational osteotomy and distal tuberosity transfer for patella subluxation secondary to excessive external tibial torsion: surgical technique and clinical outcome. *Knee surgery, sports traumatology, arthroscopy : official journal of the ESSKA* 22(11):2682–2689. <https://doi.org/10.1007/s00167-013-2561-5>
- Imhoff FB, Cotic M, Liska F, Dyma FGE, Beitzel K, Imhoff AB, Herbst E (2019) Derotational osteotomy at the distal femur is effective to treat patients with patellar instability. *Knee surgery, sports traumatology, arthroscopy : official journal of the ESSKA* 27(2):652–658. <https://doi.org/10.1007/s00167-018-5212-z>
- Lee SY, Jeong J, Lee K, Chung CY, Lee KM, Kwon SS, Choi Y, Kim TG, Lee JI, Lee J, Park MS (2014) Unexpected angular or rotational deformity after corrective osteotomy. *BMC Musculoskelet Disord* 15:175. <https://doi.org/10.1186/1471-2474-15-175>
- Nelitz M, Wehner T, Steiner M, Durselen L, Lippacher S (2014) The effects of femoral external derotational osteotomy on frontal plane alignment. *Knee surgery, sports traumatology, arthroscopy : official journal of the ESSKA* 22(11):2740–2746. <https://doi.org/10.1007/s00167-013-2618-5>
- Imhoff FB, Scheiderer B, Zakko P, Obopilwe E, Liska F, Imhoff AB, Mazzocca AD, Arciero RA, Beitzel K (2017) How to avoid unintended valgus alignment in distal femoral derotational osteotomy for treatment of femoral torsional malalignment - a concept study. *BMC Musculoskelet Disord* 18(1):553. <https://doi.org/10.1186/s12891-017-1904-7>
- Jud L, Vlachopoulos L, Haller TV, Fucntese SF, Rahm S, Zingg PO (2020) The impact of mal-angulated femoral rotational osteotomies on mechanical leg axis: a computer simulation model. *BMC musculoskeletal disorders* 21(1):50. <https://doi.org/10.1186/s12891-020-3075-1>
- Jacquet C, Chan-Yu-Kin J, Sharma A, Argenson JN, Parratte S, Ollivier M (2018) More accurate correction using “patient-specific” cutting guides in opening wedge distal femur varization osteotomies. *Int Orthop*. <https://doi.org/10.1007/s00264-018-4207-1>
- Munier M, Donnez M, Ollivier M, Flecher X, Chabrand P, Argenson JN, Parratte S (2017) Can three-dimensional patient-specific cutting guides be used to achieve optimal correction for high tibial osteotomy? Pilot study. *Orthopaedics & traumatology, surgery & research : OTSR* 103(2):245–250. <https://doi.org/10.1016/j.otsr.2016.11.020>
- Shi J, Lv W, Wang Y, Ma B, Cui W, Liu Z, Han K (2019) Three dimensional patient-specific printed cutting guides for closing-wedge distal femoral osteotomy. *Int Orthop* 43(3):619–624. <https://doi.org/10.1007/s00264-018-4043-3>
- Waidelich HA, Strecker W, Schneider E (1992) Computed tomographic torsion-angle and length measurement of the lower extremity. The methods, normal values and radiation load. *RoFo : Fortschritte auf dem Gebiete der Rontgenstrahlen und der Nuklearmedizin* 157(3):245–251. <https://doi.org/10.1055/s-2008-1033007>
- Goutallier D, Van Driessche S, Manicom O, Sariali E, Bernageau J, Radier C (2006) Influence of lower-limb torsion on long-term outcomes of tibial valgus osteotomy for medial compartment knee osteoarthritis. *J Bone Joint Surg Am* 88(11):2439–2447. <https://doi.org/10.2106/JBJS.E.01130>
- Vlachopoulos L, Schweizer A, Graf M, Nagy L, Fürnstahl P (2015) Three-dimensional postoperative accuracy of extra-articular forearm osteotomies using CT-scan based patient-specific surgical guides. *BMC Musculoskelet Disord* 16:336. <https://doi.org/10.1186/s12891-015-0793-x>
- Murase T, Oka K, Moritomo H, Goto A, Yoshikawa H, Sugamoto K (2008) Three-dimensional corrective osteotomy of malunited fractures of the upper extremity with use of a computer simulation system. *J Bone Joint Surg Am* 90(11):2375–2389. <https://doi.org/10.2106/JBJS.G.01299>
- Schweizer A, Fürnstahl P, Harders M, Szekeley G, Nagy L (2010) Complex radius shaft malunion: osteotomy with computer-assisted planning. *Hand (N Y)* 5(2):171–178. <https://doi.org/10.1007/s11552-009-9233-4>
- Wu G, Siegler S, Allard P, Kirtley C, Leardini A, Rosenbaum D, Whittle M, D’Lima DD, Cristofolini L, Witte H, Schmid O, Stokes I, Standardization, Terminology Committee of the International Society of B (2002) ISB recommendation on definitions of joint coordinate system of various joints for the reporting of human joint motion—part I: ankle, hip, and spine. *International Society of Biomechanics. J Biomech* 35(4):543–548
- Schneider P, Eberly DH (2002) Geometric tools for computer graphics. **MorganKaufmann**
- Fürnstahl P, Schweizer A, Graf M, Vlachopoulos L, Fucntese S, Wirth S, Nagy L, Szekeley G, Goksel O (2016) Surgical treatment of long-bone deformities: 3D preoperative planning and patient-specific instrumentation. *Computational radiology for orthopaedic interventions*. Springer, New York, pp 123–149
- Landis JR, Koch GC (1977) The measurement of observer agreement for categorical data. *Biometrics* 33:159–174
- Fiz N, Delgado D, Sanchez X, Sanchez P, Bilbao AM, Oraa J, Sanchez M (2017) Application of 3D technology and printing for femoral derotation osteotomy: case and technical report. *Annals of translational medicine* 5(20):400. [Doi:https://doi.org/10.21037/atm.2017.07.03](https://doi.org/10.21037/atm.2017.07.03)
- Dobbe JG, Pre KJ, Kloen P, Blankevoort L, Streekstra GJ (2011) Computer-assisted and patient-specific 3-D planning and evaluation of a single-cut rotational osteotomy for complex long-bone deformities. *Medical & biological engineering & computing* 49(12):1363–1370. <https://doi.org/10.1007/s11517-011-0830-3>
- Kolp D, Ziebarth K, Slongo T (2017) Rotation or derotation osteotomy of the tibia. *Operative Orthopädie und Traumatologie* 29(2):163–172. <https://doi.org/10.1007/s00064-016-0473-5>
- Rathey T, Hyndman J (1994) Rotational osteotomies of the leg: tibia alone versus both tibia and fibula. *J Pediatr Orthop* 14(5):615–618. <https://doi.org/10.1097/01241398-199409000-00012>
- Ryan DD, Rethlefsen SA, Skaggs DL, Kay RM (2005) Results of tibial rotational osteotomy without concomitant fibular osteotomy in children with cerebral palsy. *J Pediatr Orthop* 25(1):84–88. <https://doi.org/10.1097/00004694-200501000-00019>
- Schroter S, Ihle C, Elson DW, Dobeles S, Stockle U, Ateschrang A (2016) Surgical accuracy in high tibial osteotomy: coronal equivalence of computer navigation and gap measurement. *Knee surgery, sports traumatology, arthroscopy : official journal of the ESSKA* 24(11):3410–3417. <https://doi.org/10.1007/s00167-016-3983-7>

**Publisher’s note** Springer Nature remains neutral with regard to jurisdictional claims in published maps and institutional affiliations.